Diagnosability of Electric Machines Using Randomized Modulation Supply

Călin Ciufudean[1], Constantin Filote[1], Adrian Graur[1], Daniel Popescu[2], Camelia Petrescu[3]

[1] *"Ştefan cel Mare" University of Suceava, 9 University Str., Ro-720225, Suceava, Romania, calin@eed.usv.ro, filote@eed.usv.ro, adriang@eed.usv.ro*
[2] *Technical University of Constructions, 66 P.Protopopescu Bvd., Ro-73232, Bucharest, Romania dpopescu@instal.utcb.ro*
[3] *ICPE Electrical Engineering CO, 313 Splaiul Unirii 3, Ro-016348, Bucharest, Romania metrologie@icpe.ro*

***Abstract*-**This paper proposes a diagnosis method for electric machine faults by measuring the harmonic spectrum of stator current. In our assumption an electrical machine is excited with a randomized modulation of switching in power converters for reducing filtering requirements and acoustic noise in motor drive applications. Therefore, we propose a new approach for modelling the randomized modulation is the availability of an explicit control of time-domain performance, in addition to the possibility of shaping the power spectrum of signal of interest. The tool used here for investigating and classifying the harmonic decomposition of disturbances is the Least-Squares Prony method. Further approaches of this new method, as well as an example are also discussed.
Key words: Current harmonic spectrum, Markov chains, Least-Squares Prony method.

I. Introduction

In a very large range of applications, electrical machines are used and their failures are costly and result in significant process down time. From theory, the current flowing in an electric machine will contain only odd harmonics provided the phase impedances and voltages are balanced. Also, the third harmonics and its integer multiples are not present in the balanced circuit. The examination of the current stator spectrum from an actual machine shows that fundamental frequency component and its entire harmonics are present in the frequency spectrum. This apparent discrepancy between circuit theory and observed machine data is due to two main reasons [1], [2]. First, virtually all voltage sources (three-phase or single-phase) contain some degree of asymmetry from one-half cycle to the next. The amount of asymmetry in a sinusoidal voltage source fluctuates in time as a direct result of changes in the various, nonlinear loads drawing power from that source. Second, all electric machines contain some amount of inherent asymmetries. These asymmetries are both electrical (e.g., differences in stator winding impedances from phase to phase) and mechanical (e.g., the air gap is never perfectly symmetrical). Both types of asymmetries contribute to an impedance unbalance from phase to phase. Thus, the fundamental and its entire harmonics will be present in the stator current spectrum for all types of alternative current machines. This paper proposes a diagnosis method for electric machine faults by measuring the harmonic spectrum of stator current, and searching for changes in the stator current spectrum, compared to a baseline spectrum. These changes in spectral content are then used to identify developing faults. In order to observe changes in spectral content the electric machine is excited with a randomized modulation (modelled with Markov chains) of switching in power converters for reducing filtering requirements and acoustic noise. The parametric spectral estimation technique used in this work is one of the most popular techniques known as autoregressive spectrum estimation [2], [3]. For example, we estimate the autoregressive spectrum $S(e^{j\omega})$, of a signal y(n). A block diagram of a generic pole-zero model is shown in Fig.1.

w(n) →

$$\frac{B_z\left(e^{j\omega}\right)}{A_p\left(e^{j\omega}\right)}=\frac{\sum_{i=0}^{z} b_z(i)\cdot e^{-j\omega_i}}{1+\sum_{i=1}^{p} a_p(i)\cdot e^{-j\omega_i}}$$

→ $y_e(n)$

Fig. 1. Pole-zero signal model

In Fig.1, w(n) is the white noise, $y_e(n)$ is an estimated version of y(n), P defines the number of denominator coefficients or poles while Z defines the number of numerator coefficients or zeros. If Z = 0, there is only a constant in the numerator, the transfer function has no zeros, and the model is an all-pole or autoregressive model. It is already proven that many real-world processes including stator current are appropriately modelled by all-pole processes. The model given in Fig.1 intends to shape the spectrum of $y_e(n)$ to match that of w(n). The model coefficients are defined by $b_z(i)$ and $a_p(i)$, and after they are computed, the spectrum of $y_e(n)$ can be estimated directly from the model coefficients (1) without actually generating $y_e(n)$:

$$S(e^{j\omega}) = \frac{|b(0)|^2}{\left|1 + \sum_{i=1}^{S} a_p(i) \cdot e^{-j\omega_i}\right|} \quad (1)$$

There are many techniques available for finding the model coefficients such that $y_e(n)$ approximates w(n), here we adopted the Least Squares Prony's method. Our paper is partitioned as follows: in section 2 we describe frequency components that are different from the electrical supply frequency, and their corresponding equations that predict their location in the current stator spectrum. Section 3 describes the theoretical support of our approach regarding the randomized modulation. In section 4 we give an example of pulse width modulation governed by a Markov chain; section 5 treats the estimation of the damped exponential parameters as a polynomial factoring problem by using the least-square Prony's method. Section 6 discusses the performance analysis of the given approach applicable to induction machines, as shown in section 4.

2. Sources of Harmonic of Stator Current

An important source of harmonics injected into the stator current of an induction machine is a cyclical load torque variation. The frequencies at which these components are produced in the stator current are given by relation (2) [3]:

$$f = f_e [1 \pm m(\frac{1-S}{p/2})] \quad (2)$$

Where f_e is the fundamental supply frequency, S is the slip, p is the number of poles and m is an integer.
Other sources of stator current harmonics are eccentricities (i.g., mechanical asymmetries), which have the frequencies predicted by (2), identical to those produced by cyclical variation in load torque. Relation (1) shows that when there is no load (S = 0), many of the harmonic components are multiples of the fundamental. This makes it difficult to identify eccentricity-related faults at low level loads. As the load increases, these components move away from and become distinguishable from the harmonics of the fundamental. An additional source of current harmonics in electric machines comes from the rotor slots, which determine modifications of the air-gap permeance [2], [3]. The frequency components produced by this phenomenon are predicted by (3):

$$f_{slot} = f_e [(m_1 R \pm n_d)(\frac{1-S}{p/2}) \pm n] \quad (3)$$

Where R is the number of rotor slots, n_d is the order of the rotating eccentricity: $n_d = 0$ for a static eccentricity, while $n_d = 1$ for a dynamic eccentricity. The order of the stator magneto motive harmonic is n.
Other sources of stator current harmonics are the broken rotor bars. In the literature, there are many ways to predict the effects of broken rotor bars and one of the most common [3] is given by relation (4), where k is an integer:

$$f_{brb} = f_e [k(\frac{1-S}{p/2}) \pm s] \quad (4)$$

Bearing faults are also capable of injecting additional components into the stator current. The research in [4] provides an equation (5) for predicting some of these components. Equation (5) states the principle that the characteristic fault frequencies generated in the machine vibration will be reflected in the stator current. In (5) f_c is the characteristic fault frequencies generated in the machine vibration, and f_b is the corresponding fault component reflected into the stator current.

$$f_b = |f_e \pm m_1 \cdot f_c| \quad (5)$$

From the relations (2) ÷ (5) it is seen that the significant frequency components in the stator current originate from known sources and they can be predicted given the machine operating parameters. The sources reviewed in this section account for the majority of the significant frequency content in the stator current.

3. Switching synthesis with Markov chains

The basic synthesis in randomized modulation is to design a randomized switching procedure that minimises given criteria for spectral characteristic of f(t), while respecting time-domain behaviour constraints. Practically optimization procedure assumes the minimization of discrete spectral components (denoted as narrow-band optimization, [4]), and the minimization of signal power in a given frequency range (denoted as wide-band optimization, [5]). The case of pulse trains specified by periodic Markov chains is denoted as ergodic cyclic [4], [5]. We assume that the state of the chain goes through a sequence of n classes of states C_i , occupying a state in each class for an average time σ_i, i = 1, ..., n. The time-average autocorrelation [6] of a random process f(t) is defined as:

$$R_f(\tau) = \lim_{n\to\infty} \frac{1}{2w}\int_{-w}^{w} E[f(t)\cdot f(\tau+t)]\cdot dt \qquad (6)$$

Where the expectation E[.] refers to the whole ensemble [.].
The contribution that states the Markov chain belonging to the class C_k, with the time-averaged autocorrelation (6) is scaled by $\tau_k / \sum_{i=1}^{n} \tau_i$, where τ_i is the expected time spent in the class C_i before a transition into the class C_{i+1}. We define P as the n x n state-transition matrix, and its $(k,i)^{th}$ entry is the probability that at the next transition the chain goes to state i, given that it is currently in state k. Each row of P sums to 1; P is thus a stochastic matrix, and therefore has a single eigenvalue $\lambda_i = 1$, with corresponding eigenvector $1_n = [1\ 1\ ...\ 1]$, and all other eigenvalues with moduli strictly less than one. It can be shown [6] that after a possible remembering of the states, the matrix P for a periodic Markov chain can be written in a block-cyclic form.

$$\mathbf{P} = \begin{bmatrix} 0 & P_{12} & 0 & ... & 0 \\ 0 & 0 & P_{23} & ... & 0 \\ ... & ... & ... & ... & ... \\ 0 & 0 & 0 & ... & P_{n-1,n} \\ P_{n1} & 0 & 0 & ... & 0 \end{bmatrix}$$

Let P_P denote the product of sub matrices of P: $P_P = P_{n1}\ ...\ P_{23}\ .\ P_{12}$, and let v_i denote the vector of steady-state probabilities, conditional on the system being in class C_i. Then, we have:

$$V_i^* = v_i \cdot P_P \qquad (7)$$

The average time spent in class C_i is:

$$\tau_i = \sum_k V_k^* \cdot \tau_k \qquad (8)$$

We notice that in relation (3) the summation refers to all states in class C_i. Let $T_o = \sum_{i'1}^{n} \tau_i$ and let $\Theta_i = diag(V_i^*)$. If the first pulse belongs to the class i, then the pulse $\tau_i + \tau$ belongs to the class (i + m) / mod n, where m represents the number of transitions between pulses τ_I and $\tau_i + \tau$. We mention that the average duration of some classes may be null, which means that these classes (with corresponding states) are skipped. This approach allows us to build a simplified Markov chain model (we present this assumption, which we believe to be novel, in the next section). When we add the contribution of all classes to the average power spectrum (scaled by the relative average duration of each class), the result can be written as follows [4].

$$S(f) = \frac{1}{T_0}\left[\sum_{i=1}^{n}\frac{\tau_i}{T_0}\cdot U_i^T(f)\cdot\Theta_i U_i(f) + 2R_e\left(I_n^T\cdot S_C\cdot I_n\right)\right] + \frac{1}{T_0^2}R_e\left(I_n^T\cdot S_d\cdot I_n\right)\sum_{i=-\infty}^{\infty}\delta\left(f-\frac{i}{T^*}\right) \qquad (9)$$

Where T* is the greatest common divisor of all waveform duration, 1_n is an n x 1 vector of 1 and U_i is the vector of Fourier transforms of waveforms assigned to states in class C_i. The matrix S_C has a Toeplitz structure, with (k,i)th entry

$$S_{ck,i}(f) = \frac{\tau_i}{T_0}\cdot U_k{}^T(f)\cdot\left(I-\Lambda_k(f)\right)^{-1}\cdot\Lambda_{k,i}(f)\cdot U_i(f) \qquad (10)$$

There Λ_k is a product of n matrices: $\Lambda_k = Q_{k-1,k},...,Q_{k,k+1}$ and $\Lambda_{k,i} = Q_{k,k+1},...,Q_{i-1,i}$, where Q is a matrix n x n whose (k,i) entry is $Q_{k,i}(\sigma) = P_{k,i}\delta(\sigma-\tau_k)$. Also, the (k,i)th entry of S_d is given by relation:

$$S_{dk,i}(f) = \frac{\tau_i}{T_0}\cdot U_k^T(f)\cdot V_k\cdot(V_i)^T\cdot U_i(f) \qquad (11)$$

Analogous with the notion of truncated Markov chains with absorbing states [6], we propose a simplified model of Markov chains for random modulation. The proposed Markov chain $X^{(m)}$ has the states {m,m+1,…} aggregated into an absorbing class of states, which has transition matrix $_{(m)}T$ satisfying:

$$ {}_{(m)}T = \begin{bmatrix} {}_{(m)}P & p_m \\ 0 & 1 \end{bmatrix} \qquad (12) $$

Where $p_m = \left[\sum_{j \geq m} p_{1j}, \sum_{j \geq m} p_{2j}, ..., \sum_{j \geq m} p_{m-1,j} \right]$. Since ${}_{(m)}P$ is irreducible for all m, it follows that $X^{(m)}$ constitutes an irreducible Markov chain for all m [6]. The states {1,…,m-1} form a transient set and m is an absorbing class of states. The n-step transition probability matrix ${}_{(m)}T^n$ is given in relation (8), where ${}_{(m)}P^n = {}_{(m)}p_{ij}^{(n)} = p_{ij}(n)$.

$$ {}_{(m)}T^n = \begin{bmatrix} {}_{(m)}P^n & \left(I_m + {}_{(m)}P + {}_{(m)}P^2 + ... + {}_{(m)}P^{m-1}\right) p_m \\ 0 & 1 \end{bmatrix} \qquad (13) $$

The transition probability between realizable classes of states is 1. This probability also indicates the priorities between the states of the system.

4. Example of pulse width modulation governed by a periodic Markov chain

In this example our goal is to generate a switching function in which blocks of pulses have deterministic duty ratios: [0.5, 0.75, 0.5, 0.25]. The periodic Markov chain shown in Fig.3, with eight states divided to four classes, is an example of a solution to such a problem [6], [7]. According to the theoretical approach in the previous paragraph, we build a simplified Markov chain in Fig.4. The Markov chains in Fig.3, respectively in Fig.4 have the same transition probabilities between states S_i, i=1,…,8 of classes C_j, j=1,…,4. We notice that the Markov chain in Fig.4 is more intuitive and tidy than the one in Fig.3. The transition probabilities equal to 1 in Fig.4 are conditioned by the existence of transition probabilities between the states of different classes.

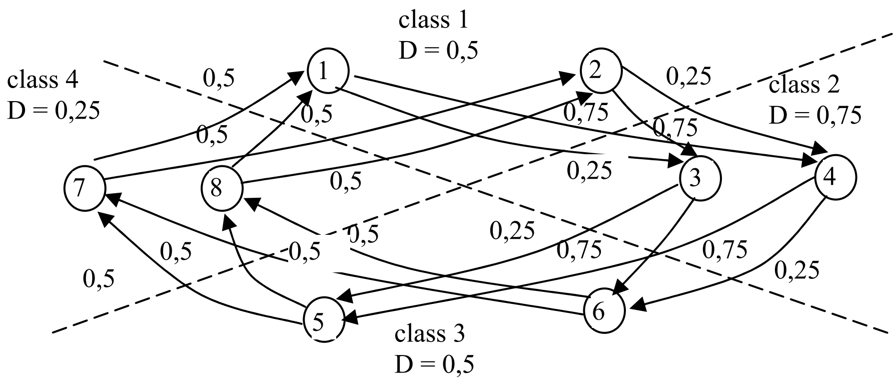

Fig.3 Classic Markov chain for modeling the switching example

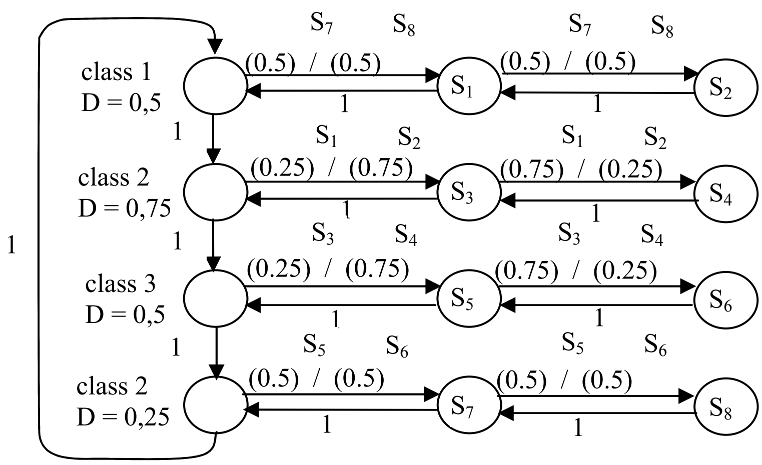

Fig.4. Proposed Markov chain for modeling the switching example

The above given duty ratios in the present example and modelled with Markov chains in Fig.3, respectively in Fig.4, represent the switching between colours red, yellow, red, green displayed by railway traffic lights commanded by data transmitter CN-75-6. We analyze this Markov chain with equation (4) and we compare the theoretical predictions with the estimates obtained in Monte Carlo simulations. The agreement between the two is quite satisfactory: the theoretical prediction for the impulse strength at f = 4 are 0.0036, and the estimated value is 0.0037. The Markov chain represented in Fig.4 allows dealing with many more classes of states because graphical representation is simplified and can significantly improve the tractability of the optimization of the Markov chains with many states.

5. Least Squares Prony Decomposition Method

As we seen in the second section, a specific source can cause a variety of disturbances which can be analyzed using various transformed domain techniques. Among these techniques a simplified approach for extracting unique wave form descriptors, which has been used in the analysis of fault-type disturbances [8], and the classification of fault type-disturbances [9], [10] is Prony's method. Prony's method decomposes the signal into a series of damped exponentials, estimating four wave forms descriptors to each disturbance: amplitude, frequency, initial phase and damping. Our approach for disturbance classification in power systems analysis involves the disturbance generation by using the pulse width modulation governed by Markov chains. We use the model given in [9], which models the disturbances as a series of damped exponentials:

$$x(n) = \sum_{k=1}^{p} B_k \cdot e^{[(b_k + j2\pi f_k)\cdot(n-1)T + j\theta_k]} \qquad (14)$$

Where B_k are the model amplitudes, p is the order of the model, b_k the damping coefficients, f_k the frequencies, Θ_k the initial phases and T is the sampling period. Prony's method [8] treats the estimation of the damped exponential parameters as a polynomial factoring matter. The discrete time series of relation (14) are:

$$x(n)' \sum_{k=1}^{p} B_k \cdot e^{j\theta_k} \cdot e^{[(b_k + j\cdot 2\pi f_k)T]^{n-1}} = \sum_{k=1}^{p} h_k \cdot z_k^{n-1} \qquad (15)$$

Where $h_k = B_k \cdot e^{j\theta_k}$ and $z_k = e^{(b_k + j\cdot 2\pi\cdot f_k)T}$.

The next step is formulating the discrete time series of equation (14) into matrix form, as follows:

$$\underline{x} = z \cdot \underline{h} \qquad (21)$$

Where: $z = \begin{bmatrix} 1 & 1 & \dots & 1 \\ z_1 & z_2 & \dots & z_p \\ \vdots & \vdots & \vdots & \vdots \\ z_1^{k-1} & z_2^{k-2} & \dots & z_p^{k-1} \end{bmatrix}$, $\underline{h} = [h_1 \ h_2 \ \dots \ h_k]^T$ and $\underline{x} = [x_1 \ x_2 \ \dots \ x_k]^{T.}$

The least squares solution to equation (21) it is: $\underline{h} = (z^H \cdot z)^{-1} \cdot z^H \cdot \underline{x}$ (22)

Having h, the amplitude and initial phase parameters for each exponential are computed using equation (23) and (24):

$$B_i = |h_i| \qquad (23)$$

$$\Theta_k = tan^{-1}[Im\{h_i\}/Re\{h_i\}] \qquad (24)$$

6. Performances Analysis

The approach presented in the previous section can examine any disturbance type (for the case of harmonics, the damping coefficients are zero). We want to test the performance of the method to injected pulse width modulated signal (with Markov chains) constructed from different voltage deviation levels. The voltage deviation level is defined as [8]:

$$x_0^* = x_0 / std(x_0) \cdot v \qquad (25)$$

Where x_0 is the injected pulse width modulated signal, v is the deviation level which represents the desired deviation in the voltage magnitude in a per unit basis, and std represents the standard deviation of a sequence. Let it be the deviation level varied from 0% - 30%. The performance is measured based on the reconstruction error, given as [9]:

$$\text{error}_{\text{reconstruction}} = \sqrt{\frac{\sum_{n=1}^{q} |x_0(n) - x(n)|^2}{q^2}} \qquad (26)$$

Where q is the length of data compared, $x_0(n)$ is the original disturbance waveform (e.g., the pulse width modulated signal), and x(n) is the reconstructed disturbance waveform. This criterion was selected since the accurate reconstruction of the waveform gives a good estimation of the waveform gives a good estimation of the waveform descriptors. A statistical measure of the technique's performance is done with 100 independent realizations for each waveform. The length of the data window used to estimate the waveforms descriptors (k) varied from 100 data points [9] (approximately 1.2 cycles)to 300 data points (approximately 4 cycles). The window of data used to estimate the parameters (k), and the window of data used to compare their performance (q), is different. The scope is focusing on a single cycle and determining the performance on a specific disturbance. Exemplifying this approach for a switching function with deterministic duty rations of blocks of pulses: [0.5, 0.75, 0.5, 0.25] (see section 4), as the deviation level increases, in the given range in section 5, our approach a good frequency and damping coefficient estimation, as summarized in Table 1.

Table 1. Performance analysis of frequency and damping coefficients

Deviation	Frequency		Damping	
[%]	Estimate [Hz]	Error	Estimate [1/sec]	Error
0	104.05568	0.00878	-0.0788	0.0057
5	104.57846	0.00854	-0.0827	0.0049
10	105.10124	0.00802	-0.0866	0.0091
15	105.62402	0.00752	-0.0905	0.0124
20	106.14680	0.00791	-0.0944	0.0258
25	106.66958	0.00857	-0.0983	0.0312
30	107.19236	0.00988	-0.1022	0.0507

From Table 1 we see that initially, both the transient frequency and transient damping coefficients are underestimated and as the deviation level increases, the estimates degrade and come closer to the actual coefficients since they were underestimated. As can be anticipated, this trend is also true as the data length increases.

7. Conclusions

This research proposes a diagnosis method for electric machine faults by measuring the harmonic spectrum of stator current. To introduce this approach, a review of sources of significant frequency components of stator current spectrum was presented. This knowledge allowed the significant fault components of electrical machines to mark theirs characteristics in the stator current harmonics configuration. We excite the electric machine with a randomized modulation of switching in power converters. Therefore we introduced a new approach for modeling the randomized Modulation with Markov Chains. The tool used to investigate and classify the harmonic decomposition of disturbances is the Least-Squares Prony method. We believe that our approach offers a new perspective for diagnosis of electrical machines and for the spectral characteristics that governs the dithering of an underlying deterministic nominal switching pattern. Further research will continue to focus in minimization of one or multiple discrete harmonics. This approach corresponds to cases where the narrow-band characteristics corresponding to discrete harmonics are harmful, as for example in the electrical machines drives.

References

[1] R. R. Obaid, T. G. Habetler, "Stator Current Analysis for Bearing Damage Detection in Induction Motors", *Proc. IEEE Int. Symp. Diagnostics for Electric Machines, Power Electronics and Drives,* pp. 182-187, 2003.

[2] J. R. Stock, T. G. Habetler, R. G. Harley, "Bearing Fault Detection via Autoregressive Stator Current Modelling", *IEEE Trans. Ind. Applicat.,* vol. 40, no. 3, pp. 740-747, 2004.

[3] R. R. Schoen, T. G. Habetler, "Effects of Time-Varying Loads on Rotor Fault Detection in Induction Machines", *IEEE Trans. Ind. Applicat.,* vol. 31, no. 6, pp. 1274-1279, 1995.

[4] G. B. Kliman, J. Stein, "Induction Motor Fault Detection via Passive Current Monitoring", *in Proc. Int. Conf. Electric Machines,* pp. 13-17, 1990.

[5] J. R. Cameron, W. T. Thomson, A. B. Dow, "Vibration and Current Monitoring for Detecting Airgap Eccentricity in Large Induction Motors", *in Proc. Inst. Electr. Eng.,* vol. 133, pp. 155-163, 1996.

[6] C. Ciufudean, C. Filote, A. Graur, G. Mahalu, "Modeling the Railway Data Transmitter CN-75-6 with Markov Chains", *in Proc. Of 1st European Conference on the Use of Modern Information and Communication Technologies,* Sient Lieven, Belgium, pp. 37-43, 2004.

[7] W. A. Wilkinson, M. D. Cox, "Discrete Warelet Analysis of Power System Transients", *IEEE Trans. On Power Systems,* vol. 11, no. 4, pp. 2038-2044, 1996.

[8] A. M. Stankovic, G. C. Verghese, D. J. Perreault, "Randomized Modulation of Power Converters via Markov Chains", *IEEE Trans. On Cont. Sys. Tech.,* vol. 5, no. 1, pp. 61-73, 1997.

[9] C. J. Dafis, C. O. Nwankapa, A. Petropulu, "Harmonic Decomposition of Transient Disturbances Using the LS Prony and ESPRIT – Based Methods", *in Proc. Of 14th PSCC,* Sevilla, Spain, Session 28, pp. 1-6, 24-28, June 2002.